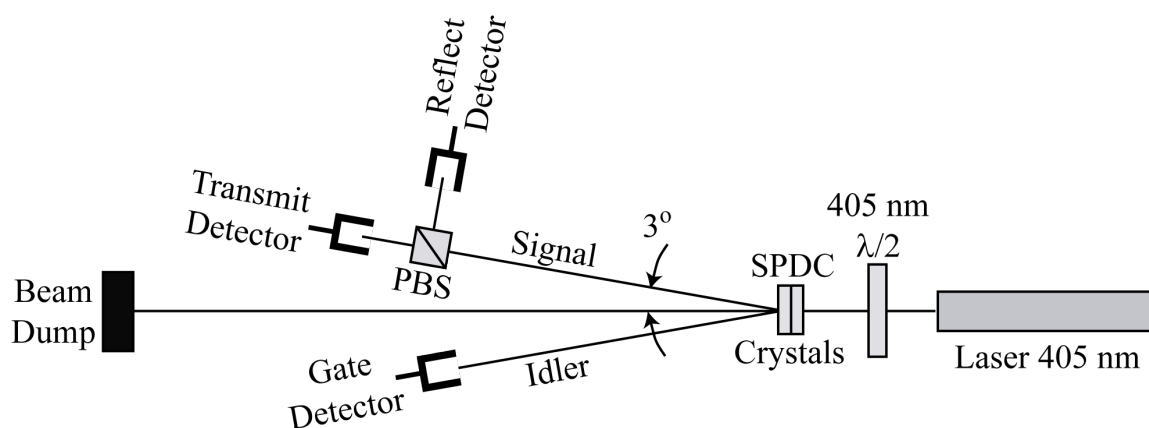*Experiment 6*

Quantum Optics

References

- *The Quantum Challenge* by G. Greenstein and A. G. Zajonc (1997, or 2nd edition 2005). The first two chapters of this book set the stage for the test of the quantum nature of light. The book as a whole is an intriguing review of recent tests of quantum theory, and suggests many elaborate experiments with our setup — tests of Bell's inequality, quantum erasers, quantum coherence theory, etc. Strongly recommended background reading!

- "The Nature of Light: What is a Photon?", *Optics and Photonics News Trends* Oct 2003. This is a special issue of *OPN Trends* focusing on the current notion of a "photon". There are five articles by renowned experts in the field of quantum optics, and the one by Arthur Zajonc and another by Rodney Loudon are particularly relevant for us.

6.1   Introduction

The particle-wave duality of light has sparked heated debate throughout the history of science. In the early 20th century, it became clear that the particle-wave duality applied to "particles" as well as light, and this of course refueled the debate leading to even deeper controversy. Not only were scientists faced with the job of reconciling in one theory the aspects of Newton's particles and Maxwell's waves, but the whole notion of physical reality as described by the new quantum theory seemed to be dragged into the fray. The Einstein-Podolsky-Rosen paradox seemed to epitomize the difficulties that many scientists encountered in constructing an appropriate view of physical reality. Quantum theory certainly seems to be successful, but the word "strangeness" is now a popular term used to describe some of its predictions — and most of these predictions have been verified experimentally!

Figure 6.1: Experimental setup for the study of the quantum nature of light. (PBS = polarizing beam splitter; SPDC = spontaneous parametric down-conversion.) According to quantum theory, a signal photon incident upon the polarizing beam splitter (PBS) is either transmitted or reflected, so no GTR triple-coincidence counts should be recorded.

The setup associated with this experiment consists of a source of entangled photon pairs, some standard optical components, and four photon-counting silicon photodetectors. (See Fig. 6.1) A wide array of measurements can be performed with this equipment, including: (1) a confirmation of the quantum nature of the photon—i.e., light exists in quanta, (2) a study of single-photon interference, (3) a demonstration that photons are bosons, (4) a test of Bell's inequalities, and (5) a demonstration of a "quantum eraser."

Beginning in the Fall of 2005 and the Spring of 2006, students in Advanced Lab and Optics Lab have performed experiment (1) and confirmed the quantum nature of the photon, though it is an experiment that has been recently enhanced by new, faster data acquisition hardware (field programmable gate array — FPGA) that makes possible new measurements with classical light sources that serve as important control experiments. The measurement exploits the properties of a pair of entangled photons and employs time-coincidence techniques to show that a photon incident upon a beam splitter is either transmitted or reflected but does *not* go in both directions as classical electromagnetic theory would predict. The experiment goes to the heart of the field of photon statistics and quantum optics.

Students have also performed experiment (4) by examining a situation in which the predictions of quantum mechanics are confirmed but those of hidden variable theories are clearly violated. The entangled polarization state of photon pairs is produced in the "spontaneous parametric down-conversion" process which forms the core of the "single photon source", a key component of the experimental setup. The experiment is very reminiscent of the Einstein-Rosen-Podolsky (EPR) paradox that started all the intellectual hubbub in the mid-20$^{\text{th}}$ century. These Bell inequality tests have been performed several times, though recently we have acquired a "precompensation" quartz crystal that should improve the "purity" of the entangled polarization

state of photon pairs and hence accentuate the failure of hidden variable theories to account for the measurements. A similar pre-compensation crystal produces highly entangled photon states in the Lynn research lab (see Julien Devin's senior thesis, 2012), but so far we have not succeeded in reproducing that result in the optics/advanced lab setup. Carefully reviewing the theory, the crystal specifications, and the experimental setup should enable us to solve this puzzle!

Finally, in the Fall of 2010, Advanced Lab students assembled an optical setup that comprises (5) a quantum eraser, and preliminary results were dramatically successful! This experiment includes an interferometer in the path of the "signal" photon which produces interference fringes, so (2) single photon interference is involved in this experiment as a delightful bonus! The measurement consists of first demonstrating fringes at the output of an interferometer in the "signal" photon path, with the polarization optics in the "idler" photon path having appropriate settings. Then a half-wave plate in the idler photon path is rotated by 22.5°, and suddenly the fringes generated in the "signal" photon path disappear because polarization now offers *which-way* information on a signal photon's path through the interferometer. When the idler half-wave plate is rotated back to its original position, the which-way information is "erased," and fringes reappear. The finges are controlled by an adjustment that is potentially space-like separated from the fringe measurement! A DC servo motor actuator has been installed to automate the collection of fringes, and fringes have been observed with the revised setup. However, the fringes do not entirely disappear, so this experiment offers the challenge of uncovering the flaw(s) in the setup and successfully observing the complete disappearance and recovery of fringes to confirm the predictions of quantum mechanics.

Choosing one of three experimental paths: You must decide which of these three types of measurements to pursue — (i) the confirmation of the quantum nature of light, (ii) tests of Bell's inequalities (with possible investigation of the pre-compensation crystal), or (iii) demonstration of a quantum eraser. You can't do all three, and you can't go wrong no matter which you choose! Each experimental path is described in more detail in a sequel document accessible wherever you found this introductory document. Enjoy the journey!

6.2   The Quantum Nature of Light

References

- "Observing the quantum behavior of light in an undergraduate laboratory," by J. J. Thorn, M. S. Neel, V. W. Donato, G. S. Bergreen, R. E. Davies, and M. Beck, *American Journal of Physics* **72**(9) 1210-1219 (2004). This paper from Mark Beck's group at Whitman College describes the experiment that Adam Pivonka and Tera Bell replicated in 2004-2005 to confirm the existence of quanta of light. In fact, Prof. Beck generously guided us as we purchased the components of our current experimental setup, and he also made available to us everything on his website, including the LabVIEW VIs that we use to acquire data. This paper is a MUST read!

- "Studying the Quantum Nature of Light," by Adam Pivonka, senior thesis, May 2005. A copy is placed with the lab reference material, and an electronic version is available on the course Sakai site. Adam describes the use of the setup to confirm the quantum nature of the photon. ALL of the details are there!

- "Comparing measurements of $g^{(2)}(0)$ performed with different coincidence detection techniques," by M. Beck, *J. Opt. Soc. Am. B* **24**, 2972-2978 (2007). This paper by Mark Beck is particularly useful if you are attempting to do a control experiment, measuring the autocorrelation function for a classical source of light. The paper explains how the limitations of our NIM counting and coincidence electronics influence the count rates and render them difficult to interpret when working with a very high single-detector rate (roughly above 50,000/s); the Whitman College group ultimately adopted FPGA data acquisition modules to overcome these limitations, and so have we! An FPGA module is available and awaits use by Optics Lab and Advanced Lab students to measure $g^{(2)}(0)$ for a classical source (as well as a single-photon source).

6.2.1   Introduction

Adam Pivonka and Tera Bell (HMC '05) pursued a study of the quantum nature of light as their senior research project. They used coincidence techniques to show that a photon incident upon a beam splitter is either transmitted or reflected, but not both at the same time! They pointed out that classical theories of the electromagnetic field cannot explain this result. In fact, even a semi-classical theory, in which atoms are quantized and the EM field is described as a classical wave, predicts a strong correlation between transmitted and reflected beams, or at least no correlation, rather than the strong anti-correlation observed (a photon counted in the transmitted beam means **no** count in the reflected beam).

The work of Adam and Tera has been repeated and confirmed by members of the Advanced Lab and Optics Lab courses, and also by Andy Fischer and Travis McQueen (HMC '06) as part of their senior thesis project. In addition, many participants in Optics Lab have conducted con-
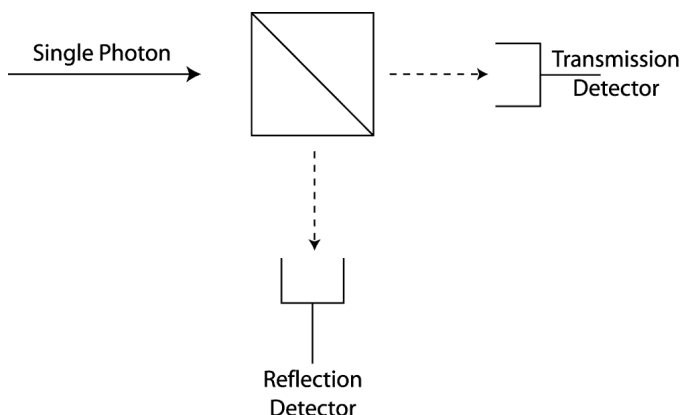
Figure 6.2: A single photon is incident upon a beam splitting cube, and photon-counting detectors look for a photon at the transmitted and reflected outputs.

trol experiments to demonstrate, as well as possible with our current NIM electronics, that our measurement scheme when applied to a classical light source yields no correlation rather than anti-correlation between the transmitted and reflected beams (see the 2007 paper by Beck). Extensive work has been performed on the data acquisition hardware in this experiment, and there is now the possibility of employing FPGA (Field Programmable Gate Array) modules to collect data with photon count rates at least 10 times higher. These higher count rates facilitate measurements of $g^{(2)}(0)$ for a classical light source with far better statistics and precision.

6.2.2 Demonstrating the Quantum Nature of Light

The conceptual scheme of our experiment is sketched in Fig. 6.2. We assume for the moment that we have a reliable source of single photons. Using this light source, we throw a steady stream of single photons at a beamsplitting cube. Photon-counting detectors are placed at the transmission and reflection outputs of the beam splitter. (See Fig. 6.3 for a photo of the experimental equipment. The detectors are housed in a light-tight box, and the photons are led to them by multimode optical fiber.) If the photon is really an indivisible particle, then either the transmission detector will record a photon, or the reflection detector will record a photon, but not both simultaneously! If the beam splitter has a 50%-50% splitting ratio, then half the time the transmission detector records the photon and half the time the reflection detector records the count. This is in sharp contrast with the classical view of this experiment.
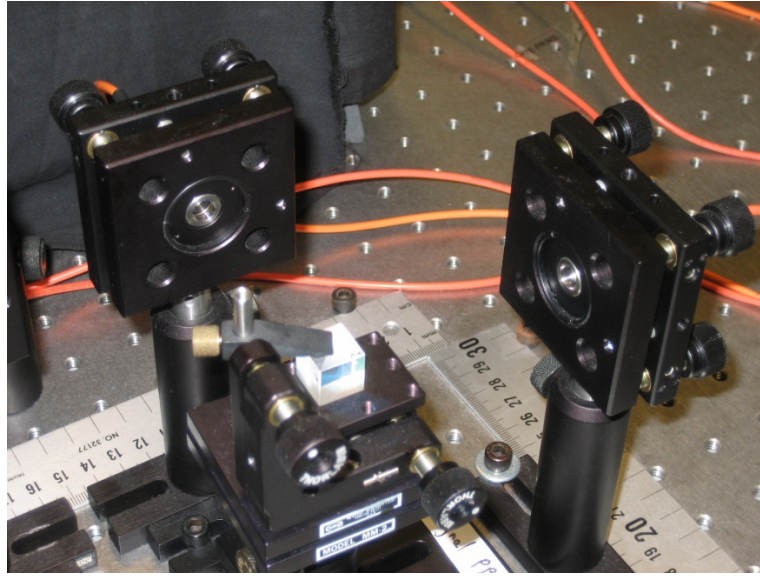
Figure 6.3: Photograph of the polarization beam splitter in the signal photon path. A vertically polarized photon incident upon the beamsplitting cube is reflected toward the "Reflect" fiber coupler, while a horizontally polarized photon is transmitted to the "Transmit" fiber coupler.

Classical Theory

The correlation between the transmitted and reflected intensities can be characterized quantitatively by the degree of second order coherence of the electric fields at the two outputs:

$$g_{TR}^{(2)}(0) = \frac{\langle I_T(t) I_R(t) \rangle}{\langle I_T(t) \rangle \langle I_R(t) \rangle} \tag{6.1}$$

We have evaluated $g_{TR}^{(2)}(\tau)$, sometimes called the "normalized intensity correlation function," at a time delay τ of zero, since we will be looking at the transmitted and reflected outputs at the same time. The angle brackets in Eq. (6.1) indicate that the time average is taken. Notice that the numerator is the time average of the product of the transmitted and reflected intensities. As mentioned above, if we do not expect the transmission and reflection detectors to produce outputs at the same time, then the numerator will be zero. In contrast, if we define transmission and reflection coefficients, T and R, then the transmitted and reflected intensities will be $I_T = T I_0$ and $I_R = R I_0$, where I_0 is the incident intensity. In our classical view, we regard the incident intensity as a continuous variable, and a portion is transmitted and a portion reflected, so that Eq. (6.1) becomes

$$g_{TR}^{(2)}(0) = \frac{\langle I_T(t) I_R(t) \rangle}{\langle I_T(t) \rangle \langle I_R(t) \rangle} = \frac{\langle T I_0(t) R I_0(t) \rangle}{\langle T I_0(t) \rangle \langle R I_0(t) \rangle} = \frac{\langle [I_0(t)]^2 \rangle}{\langle I_0(t) \rangle^2} \tag{6.2}$$

The Cauchy-Schwartz inequality implies that $\left\langle [I_0(t)]^2 \right\rangle \geq \left\langle I_0(t) \right\rangle^2$, so that classically we have

$$g_{TR}^{(2)}(0, \text{ classical}) = \frac{\langle I_T(t) I_R(t) \rangle}{\langle I_T(t) \rangle \langle I_R(t) \rangle} = \frac{\left\langle [I_0(t)]^2 \right\rangle}{\langle I_0(t) \rangle^2} \geq 1 \tag{6.3}$$

The Whitman College group (Thorn et al., 2004) and also Adam Pivonka (HMC senior thesis) have shown that Eq. (6.3) holds also in the semi-classical view. In this theory, the energy states of atoms are quantized so that energy is absorbed from the electromagnetic field in quanta, but the electromagnetic field itself is treated classically as a continuous field.

Quantum Theory

When the electromagnetic field is quantized (quantum electrodynamics or QED), the transmitted and reflected intensities in Eq. (6.1) become operators (denoted with hats)

$$g_{TR}^{(2)}(0) = \frac{\langle : \hat{I}_T \hat{I}_R : \rangle}{\langle \hat{I}_T \rangle \langle \hat{I}_R \rangle} \tag{6.4}$$

In Eq. (6.4), the colons indicate normal ordering of the creation and annihilation operators that are implicit in the intensity operators. The Whitman group and Adam Pivonka present a careful evaluation of Eq. (6.4) with the result

$$g_{TR}^{(2)}(0, \text{ quantum}) = \frac{\langle : \hat{I}_T \hat{I}_R : \rangle}{\langle \hat{I}_T \rangle \langle \hat{I}_R \rangle} = 0 \tag{6.5}$$

We shall not repeat their derivation here, but simply note that that the result agrees with our intuitive expectation that a particle-like photon will be detected by the transmission detector or by the reflection detector, but not by both at the same time.

Theory Summary

When the transmitted intensity is completely uncorrelated with the reflected intensity, the average of the product in the numerator of Eq. (6.1) is equal to the product of the averages, and $g_{TR}^{(2)}(0) = 1$. This is the case for laser sources. It is also true that photons are distributed in a laser beam such that the number of photons detected in a time interval Δt is distributed according to the Poisson distribution. (See Eq. (6.6) below.)

When the transmitted intensity is positively correlated with the reflected intensity, so that both detectors are likely to be detecting photons at the same time (in bunches), then $g_{TR}^{(2)}(0) > 1$. This is the case for "thermal" or "chaotic" sources like fluorescent lights or incandescent light bulbs. If the detectors are fast enough to follow the fluctuations of these sources, then $g_{TR}^{(2)} = 2$. In this case, the numbers of photons detected in a time interval Δt are distributed according to the Bose-Einstein distribution.

Only when the transmitted intensity is perfectly *anti*-correlated with the reflected intensity does $g_{TR}^{(2)}(0) = 0$. In this truly quantum case, the photon distribution is called "sub-Poissonian" because the variance of the number of photons detected in a time interval Δt is less than the mean number.

Single-Photon Light Sources

Up to this point we have assumed that we possess a single photon light source with which we can launch a steady stream of photons toward the beam splitting cube in Figures (6.1) and (6.2). It is tempting to imagine constructing such a light source simply by attenuating a laser beam so that, on average, only one photon is in the vicinity of the beam splitter at any given time. The probability of detecting n laser photons in a time interval Δt is given by the Poisson distribution

$$P(n, \Delta t) = \frac{\langle n \rangle^n}{n!} e^{-\langle n \rangle} \tag{6.6}$$

where $\langle n \rangle$ is the average number of photons recorded in Δt. Using Eq. (6.6), it is easy to show that the ratio of probabilities of detecting 2 photons to just 1 photon in a time interval Δt is

$$\frac{P(2, \Delta t)}{P(1, \Delta t)} = \frac{\langle n \rangle}{2} \tag{6.7}$$

If Δt is the time taken by light to travel through the vicinity of the beam splitter, and if the laser is attenuated so that $\langle n \rangle \ll 1$, then there will be usually just one photon in the vicinity of the beam splitter. However, the probability of having any photons at all in the vicinity of the beam splitter is now small, since $P(1, \Delta t) \approx \langle n \rangle \ll 1$. It is tricky to attenuate the laser just enough to be fairly certain that only one photon is in the vicinity of the beam splitter at a time, and yet not too much so that count rates are still high enough to be usable. In any case, a more fundamental objection to this strategy is that $g_{TR}^{(0)}(0)$ is normalized by the average count rates in such a way that its value would still be 1 for an attenuated laser beam! We clearly need a non-classical single-photon light source if we are to demonstrate the particle nature of the photon.

6.2.3   The Experimental Setup

Our experimental setup for studying the quantum nature of light is sketched in Fig. 6.4. The entangled photon-pair source comprises a 50-mW violet laser (405 nm) illuminating a pair of barium borate (BBO) crystals cut to facilitate type-I spontaneous parametric down-conversion (SPDC). In this nonlinear process an occasional incident 405-nm photon is converted into a pair of 810-nm photons with linear polarization orthogonal to the linear polarization of the incident beam. The two BBO crystals are cut at the same angle to their optic axes but then oriented at 90° to one another, so that the two different crystals yield SPDC photons with orthogonal polarizations. The half-wave plate provides a means for rotating the polarization of the incident beam
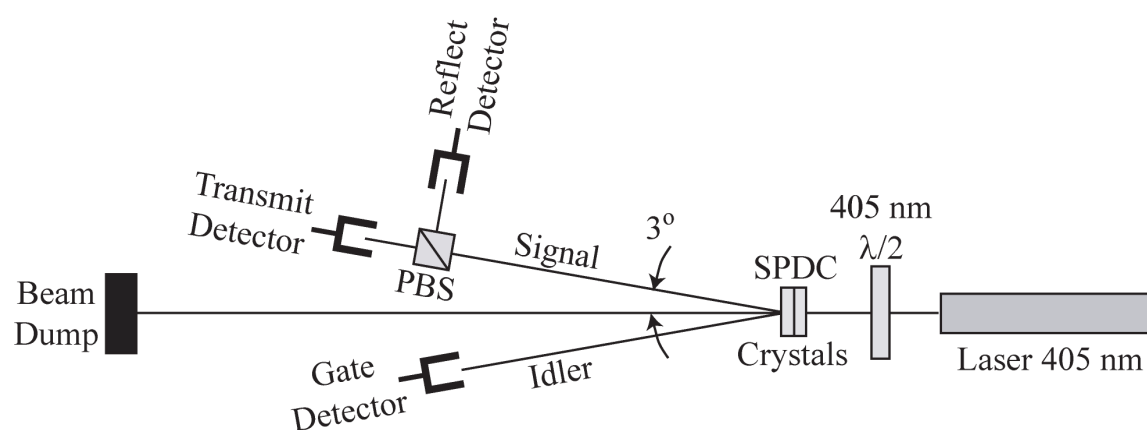
Figure 6.4: Experimental setup for the study of the quantum nature of light. (PBS = polarizing beam splitter; SPDC = spontaneous parametric down-conversion.)

so that roughly equal numbers of horizontally and vertically polarized 810-nm photons are produced in the SPDC process. Conservation of momentum and energy imposes constraints on the two 810-nm photons, so that they are entangled in energy, direction, and polarization.

One of the 810-nm photons is called the **idler** photon and is used as a gate for coincidence circuitry, while the other 810-nm photon is called the **signal** photon and is directed toward a beam splitter. In effect, gating with the idler photon allows us to conduct measurements in the signal path only when we know there happens to be a single photon in that path. This type of setup is known as an *a posteriori* source of single photons, as opposed to the desirable but technically daunting *a priori* source which would produce single photons on demand.

The idler and signal photons are captured by lens/optical-fiber combinations called "fiber couplers." The optical fiber transports the photons to silicon **avalanche photodiodes** (APDs) that are capable of detecting single photons with 60% quantum efficiency. The 20-ns-wide TTL pulses from the photodetectors are sent to three time-to-amplitude/single-channel-analyzer (TAC/SCA) modules that record two-way and three-way coincidences. The two-way coincidences are between the gate and transmission detectors (GT) and between the gate and reflection detectors (GR). The three-way coincidences involve all three detectors (GTR). See Fig. 6.5 for a schematic of electrical connections.

It is important to understand the operation of the TAC/SCA modules. In fact, setup and understanding of these may well occupy you for more than one full lab session. Let us consider the GT TAC/SCA module, in which the gate pulse is connected to the START input and the transmission pulse is connected to the STOP input. The TAC circuitry generates an output pulse with an amplitude that is proportional to the delay between the START pulse and the STOP pulse. We have inserted a little extra cable in the transmission and reflection pathways (10 ft and 20 ft, re-
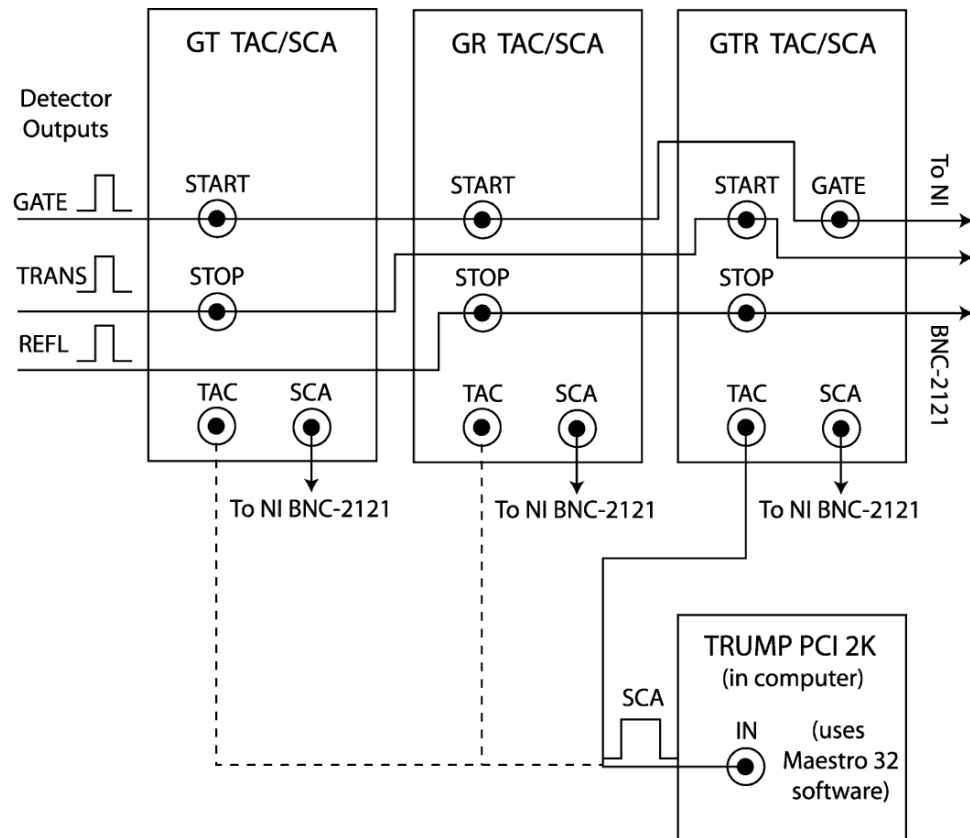
Figure 6.5: Output pulses from the three detectors are routed to three Ortec 567 Time-to-Amplitude/Single-Channel-Analyzer (TAC/SCA) modules and to the National Instruments 6602 Counter/Timer board through the BNC-2121 Connector Accessory. See Fig. 6.6 for the connections to the BNC-2121 Connector Accessory. The TAC outputs are connected to the Ortec TRUMP PCI 2K pulse height analyzer board for analysis of the timing of the photon pulses using the Maestro 32 software.

spectively) so that the transmission pulse is conveniently delayed by ~15 ns, and the reflection pulse is delayed by ~30 ns. As a result, when gate and transmitted photons are received by the detectors simultaneously, the GT TAC circuitry outputs a 3-μs-wide pulse with an amplitude of about 3.0 V (10 V corresponds to 50 ns delay, so 3 V corresponds to 15 ns). The SCA circuitry on the GT module is set so that TAC pulses ranging from 2.6 to 3.4 volts will generate an SCA output pulse (about 3-μs wide) which is then counted by the NI 6602 counter board. See Fig. 6.6 for a schematic of connections to 6 of 8 counters on the NI 6602 board. The TAC output, in addition to being passed internally to the SCA circuitry, can be sent to the TRUMP PCI 2K pulse height analyzer (PHA) card. The Maestro 32 software can be used to examine the amplitudes of TAC pulses and hence the time delays between the START and STOP pulses, and this information greatly simplifies the setting of the window of the SCA.
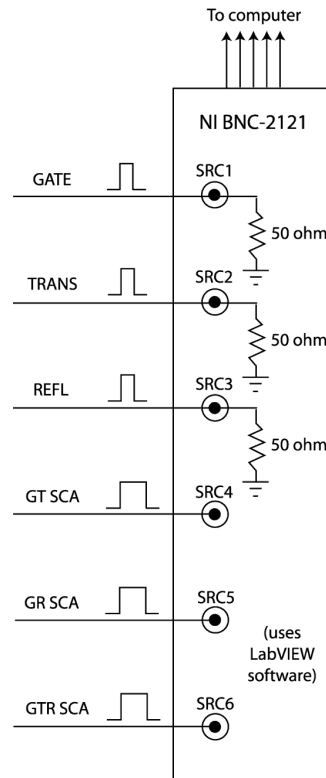
Figure 6.6: Signals are routed by the National Instruments BNC-2121 connector accessory to the National Instruments 6602 Counter/Timer Board which is inserted into the chassis of the computer. The NI 6602 has 8 counters, and we use 6 of them. The board is controlled by LabVIEW software.

How Can We Measure $g^{(2)}(0)$?

We need to relate measurable count rates to the definition of $g_{TR}^{(2)}(0)$ in Eq. (6.1). You can probably convince yourself of the following expression:

$$g_{TR}^{(2)}(0) = \frac{\langle I_T(t) I_R(t) \rangle}{\langle I_T(t) \rangle \langle I_R(t) \rangle} = \frac{P_{TR}}{P_T P_R} \tag{6.8}$$

Here P_{TR} is the probability of recording a transmitted photon and a reflected photon in the same time interval Δt, and P_T and P_R are the probabilities of recording a transmitted photon or a reflected photon in a time interval Δt, respectively. However, in order to implement our single photon source, we condition the recordings of transmitted and reflected photons on the reception of a simultaneous gate photon (idler photon). We must rewrite the expression in Eq. (6.8) so that it is relevant to our use of a single photon source, obtaining

$$g_{TR}^{(2)}(0) = \frac{\langle I_T(t) I_R(t) \rangle}{\langle I_T(t) \rangle \langle I_R(t) \rangle} = \frac{P_{GTR}}{P_{GT} P_{GR}} \tag{6.9}$$

where, for example, P_{GTR} is the probability of recording counts in all three detectors in a time interval ΔT. With a little more thought, you can probably convince yourself that these conditional probabilities can be expressed in terms of recorded counts,

$$P_{GT} = \frac{N_{GT}}{N_G} \qquad P_{GR} = \frac{N_{GR}}{N_G} \qquad P_{GTR} = \frac{N_{GTR}}{N_G} \tag{6.10}$$

where N_{GT} is the number of GT coincidence counts recorded in a given time interval, and N_G is the number of singles counts recorded by the gate detector in the same time interval. Three subscripts indicate triple coincidences. Combining Eqs. (6.9) and (6.10) we have

$$g_{TR}^{(2)}(0) = \frac{\langle I_T(t) I_R(t) \rangle}{\langle I_T(t) \rangle \langle I_R(t) \rangle} = \frac{P_{GTR}}{P_{GT} P_{GR}} = \frac{N_{GTR} N_G}{N_{GT} N_{GR}} \tag{6.11}$$

Our job then is to measure these coincidence counts and singles counts and discover if indeed our value for $g_{TR}^{(0)}(0)$ is close to zero as we would expect for a single photon source, or if it is nearer to 1.0 as we would expect from a classical perspective.

6.2.4   Measurements During the First Lab Meeting

You will want to begin your labwork by checking on optical alignment and instrument settings, and doing so will help to familiarize yourself with the experimental setup. But first a few words of caution:

> **Caution**
>
> - Wear the laser safety goggles when you turn on the blue laser
>
> - Turn off the room lights before powering on the photodetectors

The first cautionary note is for your own safety, and the second is for the protection of our photon-counting silicon avalanche photodiodes. The module of four detectors costs $12,000! On the other hand, *your eyes are priceless!!*

To begin, have your instructor or an experienced colleague show you how to mount the BBO crystals in their mirror mount. The crystals are hygroscopic (suck up moisture from the air), so we store them with desiccant in a container on the optical table when not in use. We also blow dry nitrogen gently across one face of the crystals while they are in use on the optical table. They are not severely hygroscopic, so don't stress out about it, but it is prudent to keep them in a dry atmosphere at all times. That's not too hard to do in a good lab in southern California! While your instructor or experienced colleague is still in the area, have them show you the long-pass filters and photodetector module in the light-tight box on the optical table. Then button everything up and get ready for the festivities!

Put your goggles on and pull the curtain around the experimental setup to protect others in the main lab area from stray laser reflections. Power $\boxed{\textbf{On}}$ the 405 nm laser. Adjust the BBO crystal

mirror mount so that the back-reflection of the laser goes right back on itself (centered on the iris diaphragm). This should be a small adjustment. You will probably want to check the general alignment of the optical setup — the 405 nm laser beam should pass through the center of the iris diaphragm in front of the laser, and also through the center of the iris diaphragm in front of the beam stop. But before making any adjustments to the alignment, please consult your instructor. Everything should already be fairly well aligned. If not, we will need to think carefully about how to proceed!

Power $\boxed{\textbf{On}}$ the NIM bin containing the TAC/SCA modules, and power $\boxed{\textbf{On}}$ the HP digital oscilloscope sitting on top of the NIM bin. Turn off all lights and darken the area as much as possible, and then use the flashlight to power $\boxed{\textbf{On}}$ the three power supplies for the photodetector module. You should disconnect the gate cable at the GTR TAC/SCA module and hook it up to the oscilloscope for viewing. The gate detector output should be 4 V high and about 20 ns wide. To observe the pulse successfully you will need to terminate the coax cable with 50 Ω to prevent ringing (reflections up and down the cable). Reconnect the gate cable to the GTR TAC/SCA module. Notice that the ends of the detector cables in this configuration are already terminated with 50 Ω just before they connect to the BNC-2121 input to the counter board (see Fig. 6.6).

Power $\boxed{\textbf{On}}$ the PC computer "Mehta" (Dell Dimension 3000) and login under the account name "**quantum**" and password "**photon**". There should be a few sheets of instructions placed with the experimental setup that will help you use the Maestro 32 software to check on the SCA windows, and help you use LabVIEW to record coincidence counts and singles counts. You should play around for a bit, performing reality checks. For example, you will want to block the laser beam and measure the detector dark counts. In complete darkness, these are about 300 to 400 counts/sec.

Recording Counts While Rotating the Incident Polarization A great way to check on the performance of the entire system is to rotate the 405-nm half-wave plate (see Fig. 6.4) and record the singles and coincidence counts at say, 10° increments. As the half-wave plate is rotated by θ, the plane of polarization of the laser light incident upon the BBO crystals rotates by 2θ. Hence the contributions of the two BBO crystals to the down-converted 810 nm beam varies, and their contributions have orthogonal polarization. The beam splitter in the signal photon path in Fig. 6.4 is a polarizing beam splitter, which means that vertically polarized photons are reflected and horizontally polarized photons are transmitted. So as the half-wave plate is rotated by θ, the GT and GR coincidence counts should vary as $\sin^2(2\theta)$ and $\cos^2(2\theta)$, respectively, with of course some arbitrary phase offset. The sum of GT and GR coincidence counts should be approximately constant. Use a sample variance approach to data acquisition, and fit your data rigorously to obtain a value for the reduced χ^2 goodness of fit.

A plot of your data should make it clear that our alignment is not perfect, or our photodetectors have very different quantum efficiencies (not likely). In any case, this will be valuable information for your next measurements.

6.2.5   Testing the Quantum Nature of Light

When you are finally ready to measure $g_{TR}^{(2)}(0)$ for our single-photon source, there are a couple of checks on equipment that you should perform first. Assuming you believe that photons behave like indivisible particles, you probably expect to measure no triple coincidences (GTR). There are lots of ways to measure zero. For example, you might just forget to power ON the photodetectors. That'll do it! You get the point. It is important to perform independent checks on the performance of the GTR TAC/SCA module to make sure that if there *were* triple coincidences, the GTR TAC/SCA module would record them.

Our use of the GTR TAC/SCA module is different from the GT and GR setups because for the GTR triple coincidence, we are employing the GATE input on the START circuitry. As indicated in Fig. 6.5, the idler photon pulse (gate pulse) is connected to the GATE input of the START circuitry, so that an idler photon will enable the START circuitry to register a START pulse from the transmission detector, which in turn allows a pulse from the reflection detector to register a STOP pulse and initiate TAC and SCA output pulses. We must be sure that this GATE input on the START circuitry is working properly. Also, we must be sure that the GTR SCA window is set properly to select a TAC pulse that corresponds to the actual time delay between a transmission detector pulse and a reflection detector pulse. We mentioned in Section II that we have inserted extra cabling in the transmission and reflection paths (10 ft and 20 ft, respectively) that results in a delay of ~15 ns for the transmission pulse and ~30 ns for the reflection pulse, relative to the gate pulse. That means that the reflection pulse should be delayed by ~15 ns relative to the transmission pulse. Hence we would expect to see GTR TAC pulses of ~ 3 V, and the SCA window should be centered at about 3 V.

Make Sure the GATE Input Works on the START Circuitry

Keep the gate pulse connected to the GATE input of the START circuitry and the transmission pulse connected to the START input of the GTR TAC/SCA module. However, disconnect the reflection pulse from the STOP input, and instead lead the transmission pulse through a 10 ft. cable from the START input to the STOP input (don't forget to terminate with 50 Ω). The 10 ft. cable will cause a ~15 ns delay (the electrical signals travel at about 8 inches/ns (2 x 10^8 m/s) in the coax cable). Connect the TAC output to the TRUMP PCI 2K card input, and switch the inhibit/out switch to "out" so that the TAC output is generated regardless of the SCA window. You should see the coincidence peak at about 15 ns. Also check to see that this GTT count rate is the same as the GT count rate. Replace the cabling to the original connections.

Make Sure the GTR SCA Window is Set Correctly

Disconnect the gate pulse from the GATE input of the START circuitry, and flip the associated switch to ANTI-coincidence. This effectively disables the GATE input on the START circuitry. No need to worry, we just checked to see that it works fine (see above). Now we want to set the SCA

window to select TAC pulses initiated by simultaneous receptions of photons at the transmission and reflection detectors. We have already said (above) that we expect TAC pulses of about 3 volts amplitude. But of course we really don't expect to observe simultaneous receptions of photons at the transmission and reflection detectors! So how are we going to check the SCA window? Here's the trick. Keep the transmission detector cable connected to the START input, but reroute the gate (idler) photon fiber coupler to the transmission detector by switching the fiber cable connections at the fiber connector manifold on the optical table. Now the gate photon will go to the transmission detector, and the reflected photon will go, as before, to the reflection detector. If the SPDC source is working at all, we would expect coincident gate and reflection photons. Check it out! When you're finished with this procedure, replace the connections to their original configuration.

Measure $g^{(2)}(0)$

A typical measurement consists of 60 counting periods of 10 seconds each — a total of 10 minutes. Use your own judgment. You may want to make several attempts at this measurement. It may be useful to make simultaneous measurements of count rates and the TAC spectrum from the GTR TAC/SCA module.

By now you are probably an expert on the system, and you may want to think about performing a control experiment. You can see the need for a good control — we are trying to measure zero convincingly! The FPGA module should be the best data acquisition hardware for measuring $g^{(2)}(0)$ for a classical light source, but it may have some problems, as you will see below. Robert Kealhofer and Chris Gage (both HMC '13) have written guides for the use of the FPGA module, and these guides are available in the lab and on the course Sakai site. It would also be prudent to measure $g^{(2)}(0)$ for our single-photon source using the FPGA module and compare the results with those obtained with the NIM electronics. Kaew Tinyanont and Yantao Wu, in an Optics Lab tech report in spring 2014, attempted this comparison, and their results suggest that the FPGA timing windows may be miscalibrated.
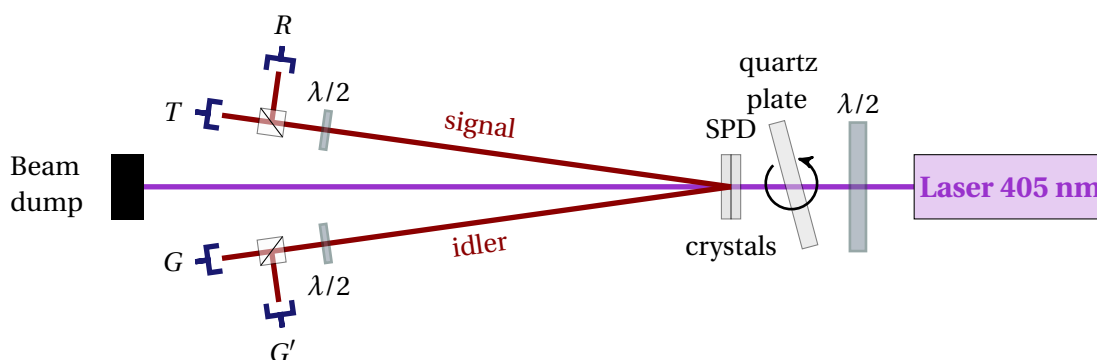
6.3   Tests of Bell's Inequality

References

- "Entangled photon apparatus for the undergraduate laboratory," and "Entangled photons, nonlocality, and Bell inequalities in the undergraduate laboratory," two papers by D. Dehlinger and M. W. Mitchell, *American Journal of Physics* **70** (9) 898-902 and 903-910 (2002). These papers focus on tests of Bell's inequalities using very much the same experimental setup as our own. Hardcopies of these papers are provided in a 3-ring binder in the lab.

- "Quantum mysteries tested: An experiment implementing Hardy's test of local realism," by J. A. Carlson, M. D. Olmstead, and M. Beck, *Am. J. Phys.* **74** (3) 180-186 (2006). Excellent guide for performing Hardy's test with our experimental setup. A hardcopy is provided in a 3-ring binder in the lab.

6.3.1   Introduction

Recent work in Advanced Lab and Optics Lab has moved beyond tests of the quantum nature of light and has focused on tests of Bell's inequality, which compares the predictions of **local hidden variable theories** with those of quantum mechanics. The papers by Dehlinger and Mitchell (*Am. J. Phys.* 2002), especially the second one (pp. 903-910), are excellent guides to these tests. With our experimental setup, tests of Bell's inequality are implemented by exploiting the polarization state of the entangled photons produced in the spontaneous parametric down-conversion (SPDC) process. Initial work in Advanced Lab and Optics Lab employed Hardy's test of local realism as described in the paper by Mark Beck's group (*Am. J. Phys.* 2006). Hardy's test is generally considered the test of Bell's theorem which is easiest to understand. However, the entangled photon states produced in our experimental setup (and in most similar setups) are only "80% pure", and this fact led to many failed attempts to use Hardy's test to demonstrate the superior predictive capabilities of quantum mechanics over hidden variable theories. During the Fall of 2009, David Berryrieser and Rob Warren (HMC '10) showed that Hardy's test could be made to work, but eventually transitioned to the more general approach of Dehlinger and Mitchell. They successfully demonstrated that quantum mechanics describes nature accurately in situations where hidden variable theories cannot. Several workers in Optics Lab have since repeated and extended the results of Berryrieser and Warren. Recently we acquired a "pre-compensation" quartz crystal which should provide 95% pure entangled photon states and a substantial improvement in our ability to rule out hidden variable theories as explanations for our measurements. Initial attempts to use the crystal have not improved the entanglement purity as much as expected (see Anthony Corso's Optics Lab tech report, spring 2014); solving this puzzle is a worthy goal for this semester!

Figure 6.7: Top view of the experimental setup for performing tests of Bell's inequalities. SPD = spontaneous parametric down-conversion. The quartz plate can be rotated about a vertical axis.

6.3.2 The Experimental Setup

The experimental setup for performing tests of Bell's inequality is sketched in Fig. 6.7 (also see photo in Fig. 6.8). The entangled photon-pair source comprises a 50 mW violet laser (405 nm) illuminating a pair of β-barium borate (BBO) crystals cut to facilitate type-I spontaneous parametric down-conversion (SPDC). In this nonlinear process an occasional incident 405-nm photon is converted into a pair of 810-nm photons with linear polarization orthogonal to the linear polarization of the incident beam. The 405-nm half-wave plate provides a means for rotating the polarization of the incident beam so that roughly equal numbers of horizontally and vertically polarized 810-nm photon pairs are produced in the SPDC process. Conservation of momentum and energy imposes constraints on the two 810-nm photons, so that they are entangled in energy, momentum, and polarization. An 810-nm photon in the bottom path of Fig. 6.7 is often called an "idler" photon and is used as a gate for coincidence circuitry, while an 810-nm photon in the top path is called the "signal" photon. In our work in testing Bell's inequality, we may refer to idler photons as "gate" photons, and the signal photons may also be called "transmit" photons. The "gate" and "transmit" nomenclature is a remnant of using this setup for the test of the quantum nature of light. In actual fact, these two paths are on an equal footing in tests of Bell's inequality, and we simply take advantage of the coincidence circuitry to measure when an entangled photon pair is transmitted successfully through the two 810-nm half-wave plates and polarizing beamsplitters.

The pair of BBO crystals in Fig. 6.7 consists of two 0.5-mm-thick crystals rotated so that their crystal axes are effectively perpendicular, and then cemented together. The result is that a horizontally polarized 405-nm photon incident upon one crystal can generate a pair of entangled 810-nm photons with their polarization vertical, while a vertically polarized 405-nm photon incident upon the other crystal can generate a pair of horizontally polarized photons. A couple of meters downstream of the BBO crystals, where the polarizers and detectors are located, it is impossible to tell in which crystal the photon pair was created because, even in principle, there

is insufficient depth resolution looking back at the BBO crystals to place the origin of the photon pair in one crystal or the other. Hence, the photons are entangled with respect to polarization as well as momentum and energy. The 405-nm laser emits horizontally polarized photons, so if the optic axis of the half-wave plate is oriented vertically (0°) (or for that matter, horizontally (90°)), a pair of vertically-polarized photons is generated. With the 810-nm $\lambda/2$ plates rotated to their 0° positions, the entangled photons will be reflected by the polarizing beamsplitters, leading to a minimum number of coincidence counts.

Why use both half-wave plates and polarizing beamsplitters, rather than polarizers to project the signal and idler photons into a particular basis? In fact, we used to use Glan-Thompson polarizers in this experiment. However, these polarizers are large and are much more likely to deviate the beams, causing a confusing decline in detection efficiency that is unrelated to polarization. By using the 810-nm $\lambda/2$ plates, you can rotate the polarization of the signal and idler photons before the polarizing beamsplitters, which reflect vertical polarization and transmit horizontal polarization. Note that each half-wave plate has a modest offset in its zero position (the idler at $-2°$ and the signal at $4°$) and that **the transmitted polarization rotates through** 2ϕ **when you rotate the wave plate by** ϕ.

The birefringent quartz plate in Fig. 6.7 provides a means of zeroing the phase φ in the QM state for the entangled photon pairs,

$$\left|\psi_{DC}\right\rangle = a|H\rangle_s|H\rangle_i + b\exp(i\varphi)|V\rangle_s|V\rangle_i \tag{6.12}$$

where normalization requires $|a|^2 + |b|^2 = 1$, and $|a|^2$ is the probability that the photon pair is polarized horizontally and $|b|^2$ is the probability of vertical polarization. The optic axis of the quartz plate is oriented vertically, so a horizontally polarized photon pair will experience a different refractive index than does a vertically polarized photon pair, and hence a phase difference is introduced between the two polarizations. Rotating the quartz plate about a vertical axis changes the effective thickness presented to the 405-nm beam, thus varying the phase difference imparted to the two polarization states. This is the method used to set $\varphi = 0$ in Eq. (6.12).

For a more detailed description of the apparatus, see the papers by Dehlinger and Mitchell and by Mark Beck's group at Whitman College (hardcopies are available in the 3-ring binders in the lab).

6.3.3   Performing Tests of Bell's Inequality

The successful completion of a test of a Bell inequality involves mastery of a number of techniques: the quantum mechanical calculations involved in predicting count rates, the calibration of the two 810-nm half-wave plates, a thorough understanding of the coincidence electronics and data acquisition equipment, and a working familiarity with the operation of the 405-nm half-wave plate and the quartz plate. The goal of our work is to perform and document successful measurements that conclude that local hidden variable theories cannot explain our experimental results while the standard theory of quantum mechanics can!
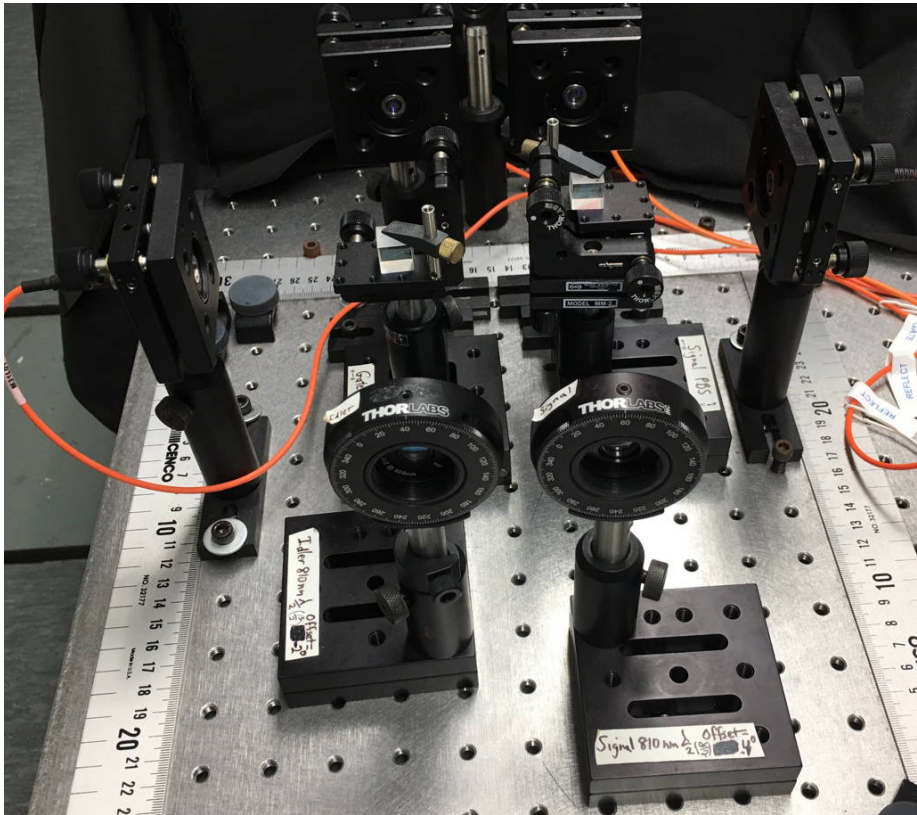
Figure 6.8: A photo of the half-wave plates, polarizing beamsplitters, and fiber couplers in the Bell inequality setup. The 405-nm laser, quartz plate, 405-nm half-wave plate, and BBO crystals (all not shown) generate 810-nm entangled photon pairs that propagate through the idler (gate) half-wave plate and polarizing beam splitter (shown on the left) and the signal (transmission) half-way plate and polarizing beamsplitter (on the right) and head toward their respective fiber couplers (face-on at the top of the photo). The 810-nm photons are carried by optical fiber to the silicon avalanche photon-counting detectors housed in the black box shown at the top of the photo.

Dehlinger and Mitchell (*Am. J. Phys.* **70** (2002) 903–910) describe in detail the procedure for performing a test of a Bell inequality first derived by Clauser, Horne, Shimony, and Holt, the so-called CHSH Bell inequality. You will need to read this paper carefully so that you understand the theory thoroughly and appreciate the motivation behind every step in their experimental procedure. A few words of advice should prove helpful and are included below.

You may want to begin by checking the orientation of the transmission axes of the signal (transmit) and idler (gate) half-wave plates. A simple method can be used to check on the settings of the two half-wave plates. With the optic axis of the 405-nm half-wave plate set vertically (actual rotation stage reading is $-1.5°$), and with the signal (transmit) half-wave plate set at 49° (45° away from its zero setting, so that it rotates vertical polarization to horizontal), rotate the idler (gate) half-wave plate while recording the signal-idler (GT) coincidence count rate. The

maximum coincidence count rate should occur at 43° (45° away from its zero setting of −2°) on the idler half-wave plate. Then with both half-wave plates set to rotate vertical polarization to horizontal, rotate the 405-nm half-wave plate to check on the reading (−1.5° ?) that gives the maximum coincidence count rate. Then rotate the signal half-wave plate to achieve a minimum GT coincidence count rate. Does it correspond to its zero position of 4°?

Hereafter, I will speak of the polarization of the signal and idler photons, rather than the settings of the 810-nm *wave plates required to achieve them.* Now rotate the 405-nm half-wave plate to achieve linear polarization at 45° to the vertical. (This should be the case when the half-wave plate rotation stage reads 21°?) Check to see that the coincidence counts $N(0°, 0°)$ and $N(90°, 90°)$ are equal. Note that Dehlinger and Mitchell define $N(\alpha, \beta)$ to be the coincidence counts when the signal (transmit) polarizer is rotated to α (taking into account any offset in the rotation stage of the polarizer) and the idler (gate) polarizer is rotated to β.

Next tune the QM state to achieve $\varphi = 0$ in Eq. (6.12), resulting in the Einstein-Podolsky-Rosen state,

$$\left| \psi_{\text{EPR}} \right\rangle = \frac{1}{\sqrt{2}} \left[|H\rangle_s |H\rangle_i + |V\rangle_s |V\rangle_i \right] \tag{6.13}$$

This is accomplished by rotating the quartz plate until the measured coincidence counts $N(45°, 45°)$ are maximized (about 30°?). You should perform the calculations to show that $\varphi = 0$ indeed corresponds to a maximum in $N(45°, 45°)$. As a double-check, you might want to confirm both theoretically and experimentally that $N(−45°, 45°)$ is a minimum when $\varphi = 0$ (looking for the minimum may be a more sensitive way to find $\varphi = 0$).

Finally, plan the sixteen measurements of coincidence counts that will allow you to evaluate S defined by (see Dehlinger and Mitchell):

$$S \equiv E(a, b) − E(a, b') + E(a', b) + E(a', b') \tag{6.14}$$

where

$$E(\alpha, \beta) \equiv \frac{N(\alpha, \beta) + N(\alpha_\perp, \beta_\perp) − N(\alpha, \beta_\perp) − N(\alpha_\perp, \beta)}{N(\alpha, \beta) + N(\alpha_\perp, \beta_\perp) + N(\alpha, \beta_\perp) + N(\alpha_\perp, \beta)} \tag{6.15}$$

and

$$a = −45° \qquad a' = 0° \qquad b = −22.5° \qquad b' = 22.5° \tag{6.16}$$

(note the misprint in Dehlinger and Mitchell, page 907, in which they erroneously say $b = 22.5°$ instead of $b = −22.5°$) and, for example,

$$\alpha_\perp = \alpha + 90° \tag{6.17}$$

You will probably find it useful to construct a table with all of the pairs of angles that you want to employ, taking account of the offsets in the readings of the rotation stages of the polarizers. Then methodically go through the sixteen measurements. Be sure to use a sample variance approach to determining your uncertainty — don't assume Poisson statistics as Dehlinger and Mitchell do, though that's probably not a bad assumption, just unnecessary!

According to the CHSH Bell inequality, $S \leq 2$, so if your calculated (measured) value of S is greater than 2 with statistical significance, then you have shown that local hidden variable theories cannot accurately describe the measurement you have performed, but presumably quantum mechanics can! The less-than-perfect purity of the state will lead to a value of $s < 2\sqrt{2} \approx 2.83$ which is the predicted value for a perfect EPR quantum mechanical state (see Eq. (6.13)).

6.4   Single Photon Interference and the Quantum Eraser

References

- "Comparing quantum and classical correlations in a quantum eraser," by A. Gogo, W. D. Snyder, and M. Beck, *Physical Review A* **71** (2005) 052103. This is an excellent paper from Mark Beck's group at Whitman College describing a quantum eraser experiment that also involves single photon interference. We should be able to repeat this experiment with our own advanced lab setup. A hardcopy of this paper is provided in a 3-ring binder in the lab.

6.4.1   Introduction

During the Fall of 2010, Advanced Lab students completed the assembly of the polarization interferometer described by Mark Beck's group in their 2005 paper (*Phys. Rev. A* **71** (2005) 052103). The interferometer was placed in the signal path of our experimental setup, and in early December, 2010, Aggie Szymanska (HMC '11) and Alex Baum (POM '11) were able to generate single photon interference fringes. Aggie and Alex did not have the benefit of motorized actuators to vary the path length difference for the two paths through the interferometer, so their achievement must be considered a true *tour de force*! They varied the path length difference manually, and in the process defined a new unit of small angular displacement, the "tiny turn"! Aggie and Alex made a valiant attempt to erase the fringes by rotating the 810-nm half-wave plate in the idler path, but the reduction in fringe amplitude was far from complete.

We now have a closed-loop motorized actuator that is capable of changing the path length difference in a precise, repeatable way, and the actuator has been installed on a kinematic mount holding the second of the two beam-displacing prisms comprising the interferometer in the signal path. During the Summer of 2011, Alex An (HMC '14) wrote a LabVIEW VI (virtual instrument) that incorporates control of the actuator into the acquisition of coincidence count rates using the NIM electronics. In Advanced Lab during the Fall of 2011, Robert Hoyt and Shaun Pacheco (HMC '12) performed some checks on the quantum eraser experimental setup, and then Susanna Todaro and Theo DuBose (also HMC '12) attempted to observe the presence or absence of single photon interference fringes to demonstrate the principles of a quantum eraser. They were unsuccessful — no fringes were observed.

In Optics Lab during the Spring of 2012, most activity focused on tests of Bell's inequality, but as a tech report project, Lucas Brady and Eric Anderson (HMC '13) took a shot at observing fringes with the quantum eraser setup. They too were unable to observe the expected fringes. Finally, in Advanced Lab during the Fall of 2012, Jesse Streitz (HMC '13) acted on a tip from Mark Beck who just happened to be visiting Mudd with his daughter. Mark suggested that the optical spectrum of the down-converted 810 nm entangled photon pairs may be broader than we thought, and hence the coherence length is shorter than we thought, so Jesse extended her search over a larger range of path length differences in the polarization interferometer in the signal arm. *Voilà!!*

Fringes were found! During the installation of the motorized actuator, the path length difference in the interferometer had been changed by about 1.5 mm, so a more aggressive scan was needed to reach the equal path length position of the interferometer. Jesse and later Robert Kealhofer (HMC '13) were able to rotate the idler 810-nm half-wave plate and significantly reduce the amplitude of the fringes, but like all their predecessors, the fringe amplitude was far from zero. In Optics Lab in the Spring 2013, the fringes were lost when the motorized actuator was bumped, but Alex An (HMC '14) and Carola Purser (HMC '13) managed to find them once again! Like researchers before them, Alex and Carola were not able to cleanly zero the fringes by adjusting the idler 810-nm half-wave plate. Clearly there remains a challenge to be answered, and the key may be in the relative numbers of horizontally versus vertically polarized entangled photon pairs. Alex An continued his work in the fall of 2013, and began to identify several polarization-sensitive elements in the beam path that may be responsible for the problem. We are close to a working quantum eraser, but still a bit of work to do! In the next section we will describe the experimental setup in more detail, and explain how the setup constitutes a quantum eraser!

6.4.2   The Experimental Setup

The experimental setup for generating single photon interference fringes is sketched in Fig. 6.9. The entangled photon-pair source is comprised of a 50-mW violet laser (405 nm) illuminating a pair of beta-barium borate (BBO) crystals cut to facilitate type-I spontaneous parametric down-conversion (SPDC). In this nonlinear process an occasional incident 405-nm photon is converted into a pair of 810-nm photons with linear polarization orthogonal to the linear polarization of the incident beam. The 405-nm half-wave plate provides a means for rotating the polarization of the incident beam so that roughly equal numbers of horizontally and vertically polarized 810-nm photons are produced in the SPDC process. Conservation of momentum and energy imposes constraints on the two 810-nm photons, so that they are entangled in energy, momentum, and polarization. An 810-nm photon in the bottom path of Fig. 6.9 is often called an "**idler**" photon and is used as a gate for coincidence circuitry, while an 810-nm photon in the top path is called the "**signal**" photon. In our work in producing single photon interference fringes, we may refer to idler photons as "gate" (G) or "gate-prime" (G') photons, depending on which detector receives them in the idler path. The signal photons may also be called "transmit" or "reflect" photons, depending on which detector receives them in the signal path. The "gate" and "transmit" and "reflect" nomenclature is a remnant of using this setup for the test of the quantum nature of light.

The pair of BBO crystals (SPDC crystals) in Fig. 6.9 consists of two 0.5-mm-thick crystals rotated so that their crystal axes are effectively perpendicular, and then cemented together. The result is that a horizontally-polarized 405-nm photon incident upon one crystal can generate a pair of entangled 810-nm photons with their polarization vertical, while a vertically polarized 405-nm photon incident upon the other crystal can generate a pair of horizontally-polarized photons. A couple of meters down-stream of the BBO crystals, where the detectors are located, it is impossible to tell where the photon pair was created because, even in principle, there is insufficient
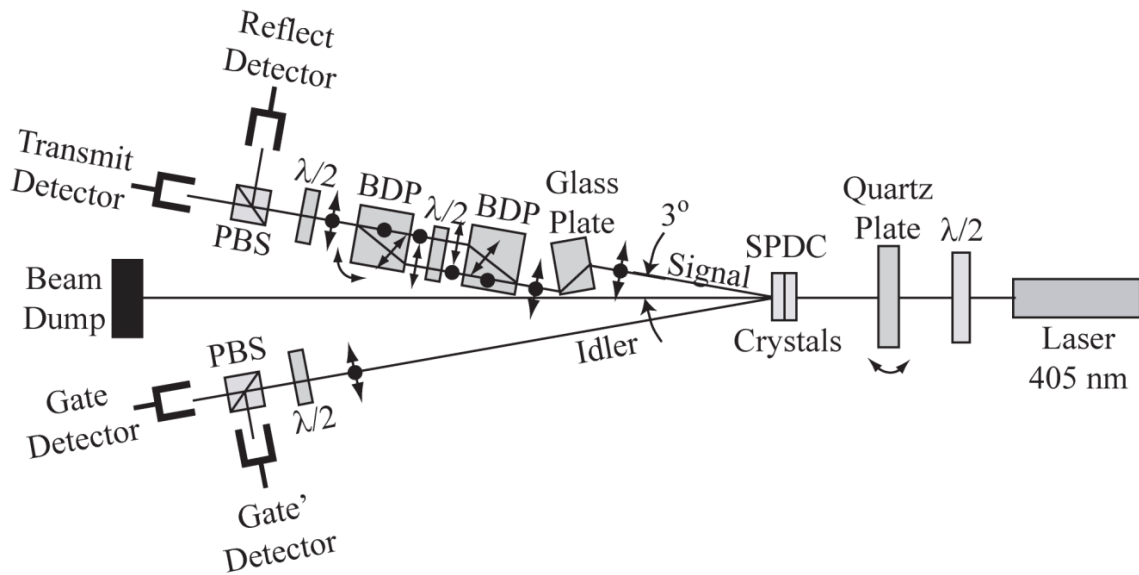
Figure 6.9: Top view of the experimental setup for generating single photon interference fringes and demonstrating the principles of a quantum eraser. The quartz plate can be rotated about a vertical axis to zero the phase φ in the QM state for the entangled photon pairs. SPDC = spontaneous parametric down-conversion. BDP = beam-displacing prism. The second beam-displacing prism (BDP) in the signal path can be rotated about a vertical axis to generate interference fringes. PBS = polarizing beam splitter.

depth resolution looking back at the BBO crystals to place the origin of the photon pair in one crystal or the other. Hence the photons are entangled with respect to polarization as well as momentum and energy.

The 405-nm laser emits horizontally-polarized photons, so if the optic axis of the 405-nm half-wave plate is oriented vertically (0°)—or for that matter, horizontally (90°)—a pair of vertically polarized 810-nm photons is generated. If the optic axis of the 405-nm half-wave plate is oriented at 45° so that the polarization of the incident laser is rotated to vertical, then a pair of horizontally polarized 810-nm photons is generated.

The birefringent quartz plate in Fig. 6.9 provides a means of zeroing the phase φ in the QM state for the entangled photon pairs:

$$\left|\psi_{DC}\right\rangle = a\left|H\right\rangle_s\left|H\right\rangle_i + b\exp\left(i\varphi\right)\left|V\right\rangle_s\left|V\right\rangle_i \tag{6.18}$$

where normalization requires $|a|^2 + |b|^2 = 1$, and $|a|^2$ is the probability that the photon pair is polarized horizontally and $|b|^2$ is the probability of vertical polarization. The optic axis of the quartz plate is oriented vertically, so a horizontally polarized photon pair will experience a different refractive index than does a vertically polarized photon pair, and hence a phase difference is introduced between the two polarizations. Rotating the quartz plate about a vertical axis changes the
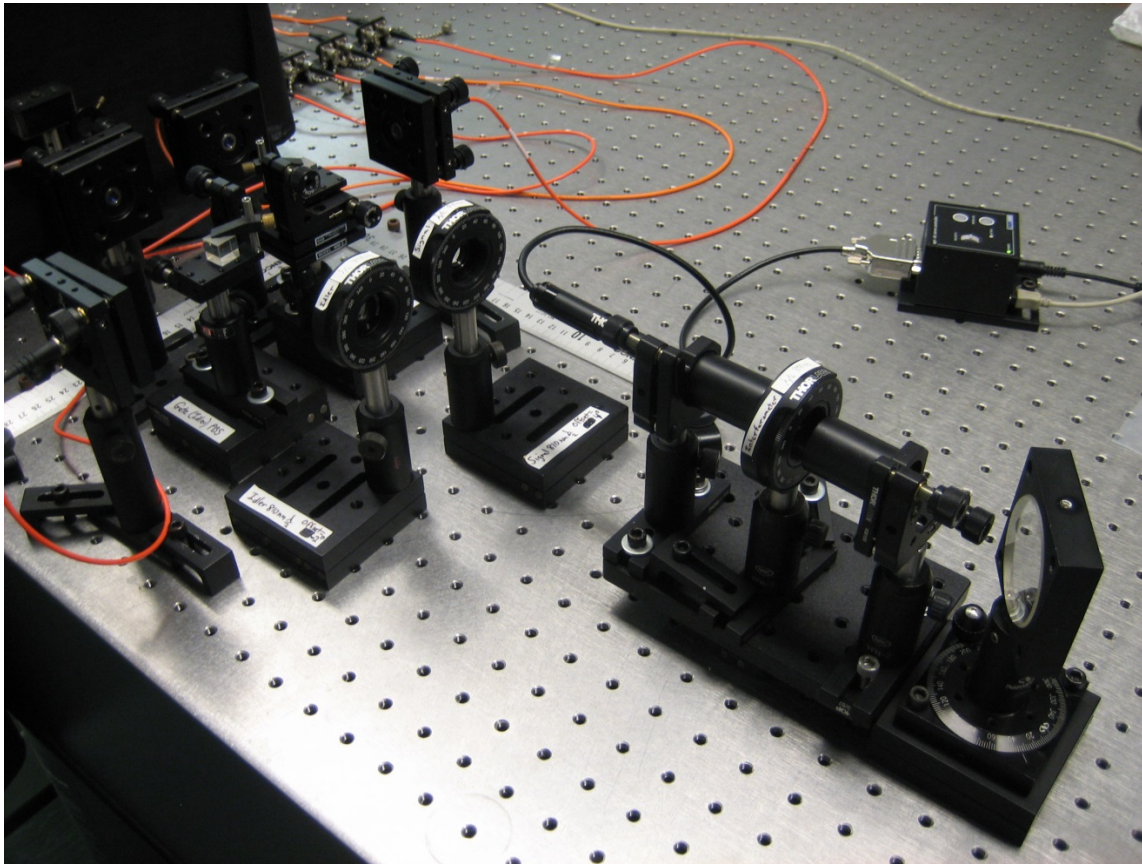
Figure 6.10: Photo of the idler (left) and signal (right) paths. The idler path consists of the 810-nm half-wave plate and the polarizing beam splitter (PBS) followed by the G (transmission) and G' (reflection) fiber coupler/photodectors. The signal path consists of the glass plate, the polarization interferometer (beam displacing prism, 810-nm half-wave plate, beam displacing prism), 810-nm half-wave plate, and PBS followed by the T (transmission) and R (reflection) fiber couplers/photodetectors.

effective thickness presented to the 405-nm beam, thus varying the phase difference imparted to the two polarization states. This is the method used to set $\varphi = 0$ in Eq. (6.18).

The polarization interferometer Two beam-displacing prisms (BDP) and an 810-nm half-wave plate form a polarization interferometer in the signal photon path. The first BDP encountered by a signal photon deflects horizontally polarized photons (denoted with a double-arrowed line in the plane of Fig. 6.10) so that they emerge from the prism at a spatially separated position from the vertically polarized photons (solid dot in Fig. 6.10). Next the 810-nm half-wave plate, whose optic axis is oriented at 45° from the vertical, converts the horizontally polarized photons to vertically polarized photons, and converts vertically po-

larized photons to horizontally polarized photons. As a result, the second BDP brings the two polarized beams back together again. The beams are now colinear, but cannot interfere because they are orthogonally polarized. The second 810-nm half-wave plate, if oriented with its optic axis at 22.5° from the vertical, will rotate the polarization of both beams by 45°. The polarizing beam-splitter (PBS) in the signal photon path will now select the vertical (horizontal) components of both beams and allow them to interfere on the reflect (transmit) detector.

The glass plate in the signal photon path introduces a displacement of the photons that compensates for the displacement introduced by the polarization interferometer. The net zero displacement allows the polarizing beam splitter and detectors to remain in the same positions they would occupy if the experimental setup is used to explore the quantum nature of light or to test Bell's inequality.

Generating single photon interference fringes If the polarization (horizontal vs. vertical) of the signal photon is unknown, even in principle, so that the signal photon takes both paths through the interferometer, then fringes can be generated by recording the coincidence count rate of the gate and transmit detectors (GT) as the second BDP is rotated about a vertical axis, thus changing slightly the path difference between the paths through the interferometer. Actually, the coincidence count rates GR or $G'R$ or $G'T$ could be recorded for the same purpose.

Which-way information and the quantum eraser If the 810-nm half-wave plate in the idler photon path has its optic axis rotated to 22.5° from vertical, then an incoming diagonally (antidiagonally) polarized photon has its polarization rotated to vertical (horizontal) before it hits the polarizing beam splitter. Thus the detection of a photon by the gate-prime (G') or gate (G) detector indicates that the idler photon was originally diagonally or antidiagonally polarized. This provides no information on the idler photon's polarization in the horizontal/vertical basis, and thus does not reveal whether the *signal* photon is horizontally or vertically polarized. Therefore, both paths through the interferometer will be explored. For this orientation of the idler half-wave plate, fringes will be observed in the records of the GT or GR or $G'T$ or $G'R$ coincidence count rates as the second BDP in the signal path is rotated about a vertical axis.

However, if the 810-nm half-wave plate in the idler path has its optic axis oriented vertically (or horizontally), then a count in the gate detector indicates horizontal polarization of the idler AND signal photons, and fringes will not be recorded. Similarly a count in the gate-prime detector indicates vertical polarization of the idler AND signal photons, and fringes will not be recorded.

Therefore, simply rotating the idler 810-nm half-wave plate by 22.5° will cause the fringes to appear or disappear, even though the G and G' detectors might, in principle, be located very far from the T and R detectors. When the idler 810-nm half-wave plate is oriented vertically, the signal photon polarization provides which-way information and no fringes are observed. When the idler 810-nm half-wave page is rotated by 22.5°, the which-way

information is "erased" and fringes are recovered — in the other arm of the setup! This is the spooky action-at-a-distance exhibited by quantum correlations in these entangled photon states.

For a beautiful and somewhat more detailed description of the apparatus and its behavior as a quantum eraser, see the paper (Gogo et al. 2005) by Mark Beck's group at Whitman College (hardcopies are available in the 3-ring binders in the lab).

6.4.3   Next Steps in Demonstrating a Quantum Eraser

Consult with your instructor to see where we are currently in acquiring data to demonstrate the complete removal of the single photon interference fringes. We suspect that a rotation of the 405-nm half-wave plate will change the relative numbers of horizontally and vertically polarized entangled photon pairs, and may make it possible to eliminate the fringes completely. We'll see! Other ideas and insights are welcome!!